0026-895X/04/6504-944–952$20.00
MOLECULAR PHARMACOLOGY
Copyright © 2004 The American Society for Pharmacology and Experimental Therapeutics
Mol Pharmacol 65:944–952, 2004

Vol. 65, No. 4
3049/1139063
Printed in U.S.A.

Analogs of α-Conotoxin MII Are Selective for α6-Containing Nicotinic Acetylcholine Receptors

J. Michael McIntosh, Layla Azam, Sarah Staheli, Cheryl Dowell, Jon M. Lindstrom, Alexander Kuryatov, James E. Garrett, Michael J. Marks, and Paul Whiteaker

Departments of Psychiatry (J.M.M.) and Biology (J.M.M., L.A., S.S., C.D.), University of Utah, Salt Lake City, Utah; University of Pennsylvania Medical School, Philadelphia, Pennsylvania (J.M.L., A.K.); Cognetix, Inc., Salt Lake City, Utah (J.E.G.); and Institute for Behavioral Genetics, University of Colorado, Boulder, Colorado (M.J.M., P.W.)

Received October 20, 2003; accepted January 7, 2004

This article is available online at http://molpharm.aspetjournals.org

ABSTRACT

Neuronal nicotinic acetylcholine receptors (nAChRs) both mediate direct cholinergic synaptic transmission and modulate synaptic transmission by other neurotransmitters. Novel ligands are needed as probes to discriminate among structurally related nAChR subtypes. α-Conotoxin MII, a selective ligand that discriminates among a variety of nAChR subtypes, fails to discriminate well between some subtypes containing the closely related α3 and α6 subunits. Structure-function analysis of α-conotoxin MII was performed in an attempt to generate analogs with preference for α6-containing [α6* (asterisks indicate the possible presence of additional subunits)] nAChRs. Alanine substitution resulted in several analogs with decreased activity at α3* versus α6* nAChRs heterologously expressed in *Xenopus laevis* oocytes. From the initial analogs, a series of mutations with two alanine substitutions was synthesized. Substitution at His9 and Leu15 (MII[H9A;L15A]) resulted in a 29-fold lower IC_{50} at α6β4 versus α3β4 nAChRs. The peptide had a 590-fold lower IC_{50} for α6/α3β2 versus α3β2 and a 2020-fold lower IC_{50} for α6/α3β2β3 versus α3β2 nAChRs. MII[H9A;L15A] had little or no activity at α2β2, α2β4, α3β4, α4β2, α4β4, and α7 nAChRs. Functional block by MII[H9A;L15A] of rat α6/α3β2β3 nAChRs (IC_{50} = 2.4 nM) correlated well with the inhibition constant of MII[H9A;L15A] for [^{125}I]α-conotoxin MII binding to putative α6β2* nAChRs in mouse brain homogenates (K_i = 3.3 nM). Thus, structure-function analysis of α-conotoxin MII enabled the creation of novel selective antagonists for discriminating among nAChRs containing α3 and α6 subunits.

nAChRs activated by the endogenous neurotransmitter acetylcholine belong to the superfamily of ligand-gated ion channels that also includes $GABA_A$, 5-hydroxytryptamine-3, and glycine receptors (Changeux, 1993). These different ligand-gated ion channels show considerable sequence and structural homology. Each of the subunits has a relatively hydrophilic amino terminal half (~200 amino acids) that constitutes an extracellular domain. This is followed by three hydrophobic transmembrane domains, a large intracellular loop, and then a fourth hydrophobic transmembrane span.

A large number of genes have been cloned that encode subunits of nAChRs. It has been proposed that these subunits may be divided into subfamilies on the basis of both gene structure and mature protein sequence. The subunits α2, α3, α4, and α6 belong to subfamily III, tribe 1; β2 and β4 belong to tribe III-2; and the putative structural subunits α5 and β3 belong to tribe III-3 (Corringer et al., 2000). Within tribe III-1, subunits α3 and α6 show considerable sequence identity (~80% in the ligand-binding extracellular domain). Thus, designing ligands to distinguish between α3*[1] and α6* is particularly challenging.

α-Conotoxin MII is a 16 amino acid peptide originally isolated from the venom of the marine snail *Conus magus*. This peptide potently targets neuronal in preference to the muscle subtype of nicotinic receptor with high affinity for both α3β2 and α6* nAChRs. Unfortunately, α-conotoxin MII may not distinguish well between α3* and α6* nAChRs (Kuryatov et al., 2000). In an effort to remedy this situation and produce a selective ligand for α6* nAChRs, we have generated a series of α-conotoxin MII analogs.

The α6 subunit is expressed in catecholaminergic neurons and in retina (Le Novère et al., 1996, 1999; Vailati et al., 1999). In striatum, α6* nAChRs seem to play a central role in the modulation of dopamine release. Recently, homozygous null mutant (α6−/−) mice were generated. Receptor autora-

This work was supported by National Institutes of Health grants MH53631, GM48677, DA12242, and NS11323.

[1] Asterisks indicate the possible presence of additional subunits.

ABBREVIATIONS: nAChR, nicotinic acetylcholine receptor; HPLC, high-performance liquid chromatography; CI, 95% confidence interval; ACh, acetylcholine.

diography studies in these animals indicate that the α6 nAChR subunit is a critical component of [^{125}I]α-conotoxin MII binding in the central nervous system (Champtiaux et al., 2002). Studies using mice with nAChR subunit deletion indicate that α3 does not participate in most [^{125}I]α-conotoxin MII binding sites but does influence expression in the habenulo-peduncular tract (Whiteaker et al., 2002). Thus, α6-selective ligands would be useful to distinguish the α6* majority form from the α3* minority of such sites.

Materials and Methods

Chemical Synthesis. Peptides were synthesized on a Rink amide resin, 0.45 mmol/g [Fmoc-Cys(Trityl)-Wang; Novabiochem, San Diego, CA] using *N*-(9-fluorenyl)methoxycarboxyl chemistry and standard side chain protection except on cysteine residues. Cysteine residues were protected in pairs with either *S*-trityl on the first and third cysteines or *S*-acetamidomethyl on the second and fourth cysteines. Amino acid derivatives were from Advanced Chemtech (Louisville, KY). The peptides were removed from the resin and precipitated, and a two-step oxidation protocol was used to selectively fold the peptides as described previously (Luo et al., 1999). Briefly, the first disulfide bridge was closed by dripping the peptide into an equal volume of 20 mM potassium ferricyanide and 0.1 M Tris, pH 7.5. The solution was allowed to react for 30 min, and the monocyclic peptide was purified by reverse-phase HPLC. Simultaneous removal of the *S*-acetamidomethyl groups and closure of the second disulfide bridge was carried out by iodine oxidation. The monocyclic peptide and HPLC eluent was dripped into an equal volume of iodine (10 mM) in H_2O/trifluoroacetic acid/acetonitrile (78:2:20 by volume) and allowed to react for 10 min. The reaction was terminated by the addition of ascorbic acid diluted 20-fold with 0.1% trifluoroacetic acid and the bicyclic product purified by HPLC.

Mass Spectrometry. Measurements were performed at the Salk Institute for Biological Studies (San Diego, CA) under the direction of Jean Rivier. Matrix-assisted laser desorption ionization time-of-flight mass spectrometry and liquid secondary ionization mass spectrometry were used.

Preparation of nAChR Subunit cRNA. Attempts to express the rat nAChR α6 subtype in *Xenopus laevis* oocytes consistently failed; that is, no ACh-gated currents were detected. To improve functional expression, we created a chimeric receptor of the rat α6 and α3 subtypes. The chimeric receptor consists of amino acids 1 to 237 of the rat α6 subunit protein linked to amino acids 233 to 499 of the rat α3 subunit protein. The chimeric junction is located at the paired -RR- residues immediately preceding the M1 transmembrane segment of the α3 subunit. The resulting chimeric receptor represents the extracellular ligand-binding domain of the α6 subunit linked to membrane-spanning and intracellular segments of the α3 subunit. The α6/α3 cDNA was constructed by the introduction of BspEI sites at the chimeric junction into the α6 and α3 cDNA sequences using mutagenic primers to introduce the restriction sites through silent codon changes. The α6 and α3 segments were generated by polymerase chain reaction of rat brain cDNA using primers in the 5′ and 3′ untranslated regions of the corresponding cDNAs along with the internal mutagenic primers. The polymerase chain reaction products were digested with BspEI and ligated to generate the chimeric construct. The final chimeric construct was cloned and completely sequenced to confirm the correct cDNA sequence. To further improve expression levels, all of the 5′ and 3′ untranslated regions of the nAChR cDNA were deleted, and the chimeric construct was cloned into the *X. laevis* expression vector pT7TS, placing *X. laevis* globin 5′ and 3′ untranslated regions around the nAChR cDNA. The expression construct pT7TS/rα6α3 was transcribed with T7 RNA polymerase to generate sense-strand RNA for oocyte expression.

Electrophysiology and Data Analysis. Clones of rat nAChR subunits were used to produce cRNA for injection into *X. laevis* oocytes as described previously (Cartier et al., 1996). The rat α6 and β3 subunits were a generous gift from S. Heinemann (Salk Institute, San Diego, CA) (Deneris et al., 1989). To express nAChRs in oocytes, 5 ng of each nAChR subunit was injected. In the case of α6β4, 50 ng of each subunit was injected because of absent expression when using 5 ng of cRNA. Likewise, 20 ng was used for the α6/α3β2 combination that expresses poorly without the β3 subunit. A 30-μl cylindrical oocyte recording chamber fabricated from Sylgard was gravity-perfused with ND96A (96.0 mM NaCl, 2.0 mM KCl, 1.8 mM $CaCl_2$, 1.0 mM $MgCl_2$, 1 μM atropine, and 5 mM HEPES, pH 7.1–7.5) at a rate of ~2 ml/min (Luo et al., 1998). All toxin solutions also contained 0.1 mg/ml bovine serum albumin to reduce nonspecific adsorption of peptide. Toxin was preapplied for 5 min. ACh-gated currents were obtained with a 2-electrode voltage-clamp amplifier (model OC-725B; Warner Instrument, Hamden, CT), and data were captured as described previously (Luo et al., 1998). The membrane potential of the oocytes was clamped at −70 mV. To apply a pulse of ACh to the oocytes, the perfusion fluid was switched to one containing ACh for 1 s. This was done automatically at intervals of 1 to 5 min. The shortest time interval was chosen such that reproducible control responses were obtained with no observable desensitization. The concentration of ACh was 10 μM for trials with α1β1δε and 100 μM for all other nAChRs. Toxin was bath-applied for 5 min, followed by a pulse of ACh. Thereafter, toxin was washed away, and subsequent ACh pulses were given every 1 min, unless otherwise indicated. All ACh pulses contain no toxin, for it was assumed that little if any bound toxin washed away in the brief time (less than the 2 s it takes for the responses to peak). In our recording chamber, the bolus of ACh does not project directly at the oocyte but rather enters tangentially, swirls, and mixes with the bath solution. The volume of entering ACh is such that the toxin concentration remains at a level >50% of that originally in the bath until the ACh response has peaked (<2 s). When longer than 5 min of toxin application was needed to reach maximum block, toxin was applied by continuous perfusion to the oocytes as described previously (Luo et al., 1994), except that ACh was applied once every 2 min.

The average peak amplitude of three control responses just preceding exposure to toxin was used to normalize the amplitude of each test response to obtain a "% response" or "% block". Each data point of a dose-response curve represents the average value ± S.E. of measurements from at least three oocytes. Dose-response curves were fit to the equation $\%\text{response} = 100/\{1 + ([\text{toxin}]/IC_{50})^{n_H}\}$, where n_H is the Hill slope determined with Prism software (GraphPad Software, San Diego, CA) on an Macintosh (Apple Computers, Cupertino, CA). For three or fewer data points, n_H was set to 1.0.

Membrane Preparation. Mice were killed by cervical dislocation. Brains were removed from the skulls and dissected on an ice-cold platform. Membranes containing [^{125}I]α-conotoxin MII binding sites were prepared from pooled olfactory tubercles, striatum, and superior colliculus. Samples were homogenized in 2× physiological buffer (288 mM NaCl; 3 mM KCl; 4 mM $CaCl_2$; 2 mM $MgSO_4$; and 40 mM HEPES, pH 7.5; 22°C) using a glass-polytetrafluoroethylene tissue grinder. Homogenates were then treated with phenylmethylsulfonyl fluoride (final concentration, 1 mM; 15 min at 22°C) to inactivate endogenous serine proteases before centrifugation (20,000*g* for 20 min at 4°C). Pellets were washed twice by homogenization in distilled deionized water glass-polytetrafluoroethylene tissue grinder, 4°C) and centrifugation (20,000*g* for 20 min at 4°C). Pooled tissue from a single mouse provided sufficient material for a single 96-well format assay.

Inhibition of [^{125}I]α-Conotoxin MII Binding. Inhibition of [^{125}I]α-conotoxin MII binding to mouse brain membranes was performed using a modified version of the 96-well plate procedure described previously (Whiteaker et al., 2000a). Assays were performed in triplicate using 1.2-ml siliconized polypropylene tubes arranged in a 96-well format. Membrane pellets were resuspended into distilled

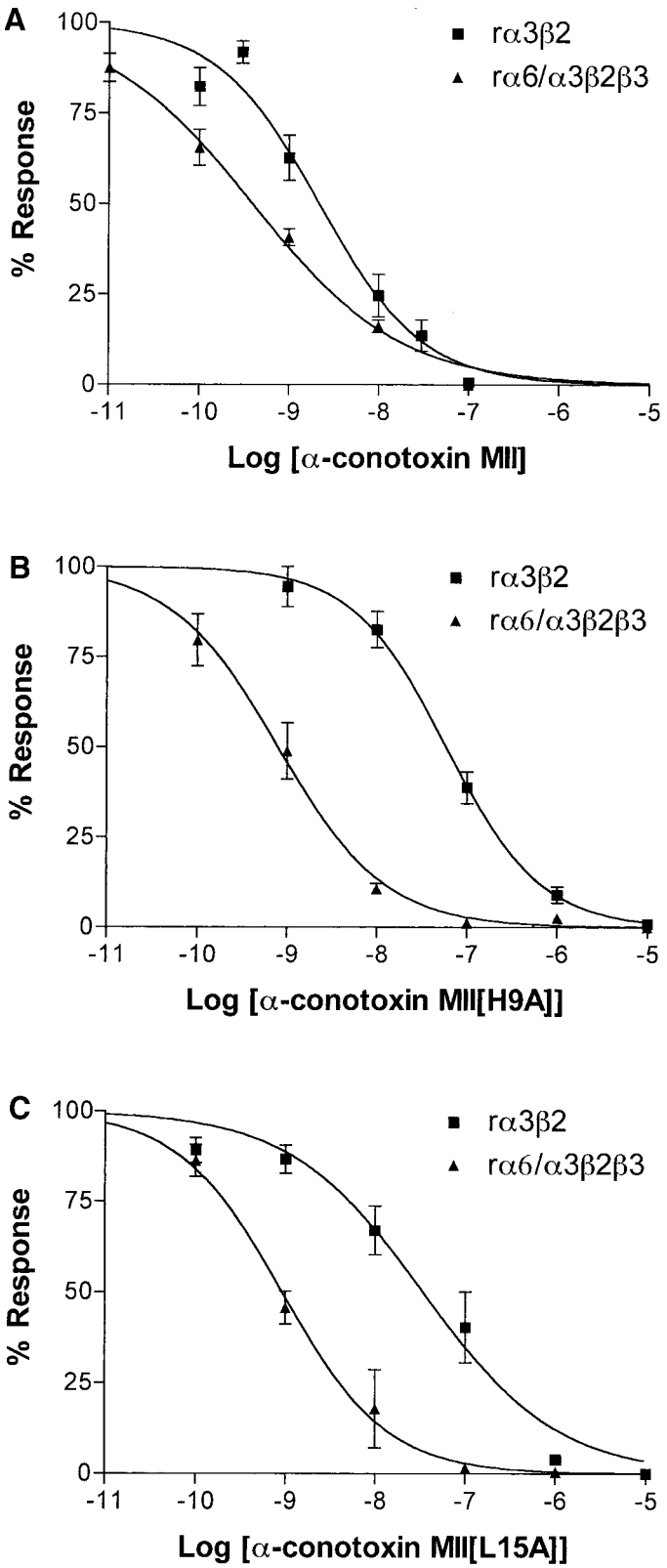

Fig. 1. H9A and L15A analogs of α-MII discriminate between α6/α3β2β3 and α3β2 nAChRs. Rat nAChR subunits were heterologously expressed in *X. laevis* oocytes. Concentration-response analysis of the peptide block of ACh-induced current was performed as described under *Materials and Methods*. α-Conotoxin MII blocked α3β2 and α6/α3β2β3 with IC_{50} values of 2.18 and 0.39 nM, respectively. See also Table 1 for confidence intervals. The Hill slopes were 0.75 ± 0.13 and 0.53 ± 0.04, respectively. MII[H9A] blocked α3β2 and α6/α3β2β3 nAChRs with IC_{50} values of 59.0 and 0.79 nM, respectively, and with Hill slopes of 0.83 ± 0.08 and 0.73 ± 0.08. MII[L15A] blocked α3β2 and α6/α3β2β3 nAChRs with IC_{50} values of 34 and 0.92 nM, respectively, and with Hill slopes of 0.58 ± 0.08 and 0.75 ± 0.08, respectively. The data are from three to six separate oocytes; ± value is the standard error of the mean.

deionized water. Total (no drug) and nonspecific (with 1 μM epibatidine) binding determinations were included in each experiment for each drug dilution series. Initial incubations proceeded for 3 h at 22°C in 1× protease inhibitor buffer [1× physiological buffer supplemented with bovine serum albumin (0.1% w/v), 5 mM EDTA, 5 mM EGTA, and 10 μg/ml each of aprotinin, leupeptin trifluoroacetate, and pepstatin A]. Each tube contained 10 μl of membrane preparation, 10 μl of competing ligand (or nonspecific or total determinations) in 1× protease inhibitor buffer, and 10 μl of [^{125}I]α-conotoxin MII (1.5 nM in 2× protease inhibitor buffer, giving a final assay radioligand concentration of 0.5 nM). After incubation, each tube was diluted with 1 ml of physiological buffer plus 0.1% (w/v) bovine serum albumin. Tubes were then incubated for a further 4 min at 22°C to reduce nonspecific binding to the membrane preparation. The binding reactions were then terminated by filtration onto a single thickness of GF/F filter paper (Whatman, Clifton, NJ) using a cell harvester (Inotech Biosystems, Rockville, MD). The filters were incubated previously for 15 min with 5% dried skim milk to reduce nonspecific binding. Assays were washed with four changes of physiological buffer supplemented with bovine serum albumin (0.1% w/v). Washes were performed at 30-s intervals, with each lasting approximately 5 s. All filtration and collection steps were performed at 4°C. Bound ligand was quantified for each filter disc by gamma counting using a Cobra II counter (≈85% efficiency) (PerkinElmer Life and Analytical Sciences, Boston, MA).

Calculations. Data from individual [^{125}I]α-conotoxin MII inhibition binding experiments were processed using a single-site fit using the nonlinear least-squares fitting algorithm of GraphPad Prism. Values of K_i were derived for each experiment by the method described by Cheng and Prusoff (1973), $K_i = IC_{50}/1 + (L/K_D)$, where K_i for [^{125}I]α-conotoxin is 0.32 nM.

Results

Peptide Synthesis. The sequence of native α-conotoxin MII is GCCSNPVCHLEHSNLC. Peptide analogs were synthesized by substituting one or more residues with alanine. These peptides are named according to the residue(s) substituted; for example, MII[E11A] has the glutamic acid in position 11 substituted with alanine. Cysteine residues were orthogonally protected to direct the formation of disulfide bonds in the configuration found in α-conotoxin MII, that is cysteine 1 to cysteine 3 and cysteine 2 to cysteine 4. The first and third cysteine residues were protected with acid-labile groups that were removed first after a cleavage from the resin; ferricyanide was used to close the first disulfide bridge. The monocyclic peptides were purified by reverse-phase HPLC. Then the acid-stable acetamidomethyl groups were removed from the second and fourth cysteines by iodine oxidation that also closed the second disulfide bridge. The fully folded peptides were again purified by HPLC. Mass spectrometry was used to confirm synthesis. The observed molecular mass for each peptide was within 0.1 Da of the expected mass.

Peptide Effects on α6* and α3* nAChRs. Injection of rat α6 subunits into oocytes either alone or in combination with β2 and/or β3 subunits yields few or no functional nAChRs. Using a previously reported strategy for human α6 (Kuryatov et al., 2000), we joined the extracellular domain of the rat α6 subunit to the transmembrane and intracellular

TABLE 1
Activity of alanine-substituted MII analogs
Numbers in parentheses are 95% confidence intervals.

Toxin	IC_{50}		
	Rat α3β2	Rat α6/α3β2β3	Ratio[a]
	nM		
MII	2.18 (1.24–3.81)	0.39 (0.281–0.548)	5.59
MII[S4A]	15.8 (7.03–35.3)	0.733 (0.513–1.05)	21.56
MII[N5A]	>10,000	793 (566–1110)	>12.6
MII[P6A]	4,420 (1880–10,400)	253 (172–372)	17.5
MII[V7A]	4.46(3.28–6.05)	10.6 (8.01–14.0)	0.421
MII[H9A]	59.0 (44.1–78.9)	0.790 (0.558–1.12)	74.7
MII[L10A]	1.47 (0.642–3.38)	0.482 (0.232–1.00)	3.05
MII[E11A]	8.72 (6.84–11.1)	0.160 (0.135–0.189)	54.5
MII[H12A]	4,660 (2420–9000)	604 (256–1420)	7.72
MII[S13A]	2.54 (1.92–3.35)	0.659 (0.450–0.966)	3.85
MII[N14A]	25.7 (17.0–38.9)	1.06 (0.742–1.52)	24.2
MII[L15A]	34.1 (19.4–59.9)	0.917 (0.657–1.28)	37.2

[a] IC_{50} α3β2/IC_{50} α6/α3/β2β3.

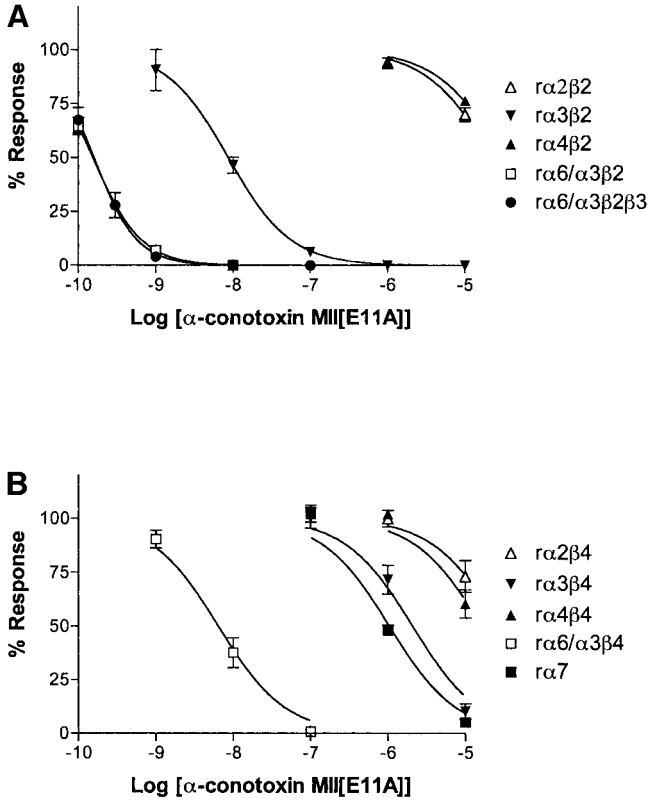

Fig. 2. Concentration-response analysis of α-conotoxin MII[E11A] on nAChR subtypes expressed in *X. laevis* oocytes. Peptide was perfusion-applied at concentrations ≤100 nM and bath-applied at higher concentrations as described under *Materials and Methods*. A, block by MII[E11A] of β2-containing nAChRs. B, block by MII[E11A] of β4-containing and α7 nAChRs. Data are from three to five oocytes. Error bars are S.E.M. Results are summarized in Table 2. Note the strong preference for α6/α3* nAChRs.

portion of the closely related rat α3 subunit. Alanine analogs were then tested against α3β2 or α6/α3β2β3 subunit combinations heterologously expressed in oocytes. The β3 subunit was used with α6/α3β2, for without it there was generally little or no functional expression. In addition, β3 is associated with native α6β2*-containing nAChRs (Zoli et al., 2002; Cui et al., 2003). Results are shown in Fig. 1 and Table 1. Substitution of alanine for Asn5, Pro6, or His12 resulted in substantially decreased activity compared with native MII at both α6* and α3* nAChRs, whereas substitution for Val7 had the most pronounced effect on the α6/α3β2β3 nAChR. Substitution for Ser4, His9, Leu10, Glu11, Ser13, Asn14, and Leu15 had only modest effects on α6/α3β2β3; however, mutations at Ser4, His9, Glu11, Asn14, and Leu15 resulted in substantially lower activity on α3β2 nAChRs. Thus, these mutations are analogs that preferentially block α6/α3β2β3 versus α3β2 nAChRs. We note that for certain analogs, including S4A, L10A, E11A, S13A, and N14A, the $t_{1/2}$ for recovery from toxin block of α6/α3β2β3 nAChRs was long (>25 min). For these analogs, 10- to 15-min toxin incubations were used to achieve maximum block at 10 nM concentration, and 20- to 35-min incubations were used to achieve maximum block at 1 nM concentration. A slow off-rate but similar affinity to other analogs implies that the analogs with a slow off-rate also have slower on-rates and thus the need for longer application times. MII[H9A] and MII[L15A] failed to block α4β2 nAChRs; at 10 μM peptide concentration, the ACh-evoked current was 105.8 ± 2.4 and 102.3 ± 5.3% of control, respectively (data from six oocytes).

TABLE 2
Activity of MII[E11A]

	IC_{50}	95% Confidence Interval	Ratio[a]
	nM		
α2β2	>10,000		>62,500
α2β4	>10,000		>62,500
α3β2	8.72	6.84–11.1	54.5
α3β4	2100	1330–3310	13,100
α4β4	>10,000		>62,500
α6/α3β2	0.154	0.134–0.178	0.962
α6/α3β2β3	0.160	0.135–0.189	1.00
α6/α3β4	6.44	4.33–9.57	40.3
α7	1051	(731–1510)	6,570

[a] nAChR subtype IC_{50}/α6/α3β2β3 IC_{50}

Selectivity of MII[E11A]. The single alanine substitution MII[E11A] has ~50-fold preference for α6/α3β2β3 versus α3β2 nAChRs and seems to be the most potent analog on α6/α3β2β3 nAChRs. We therefore tested its effects on additional nAChR subtypes. The apparent on-rate for α6/α3β4 nAChRs is slow; at concentrations of toxin ≤ 10 nM, 60 to 70 min of toxin application was required to reach a steady-state level of nAChR block. Concentration-response curves are shown in Fig. 2 and IC_{50} values are shown in Table 2.

TABLE 3
Activity of doubly substituted MII analogs
Numbers in parentheses are 95% confidence intervals.

Toxin	IC_{50}		Ratio[a]
	Rat $\alpha3\beta2$	Rat $\alpha6/\alpha3\beta2\beta3$	
	nM		
MII[S4A;H9A]	207 (156–274)	1.97 (1.31–2.97)	105
MII[H9A;L15A]	4850 (3540–6630)	2.40 (1.68–3.43)	2020
MII[L10A;L15A]	17.2 (8.11–36.6)	1.80 (1.26–2.56)	9.56
MII[E11A;L15A]	50.1 (41.4–60.6)	0.415 (0.223–0.772)	121

[a] IC_{50} $\alpha3\beta2/IC_{50}$ $\alpha6/\alpha3/\beta2\beta3$.

Double Mutants. A series of double alanine-substituted mutations was also constructed. These mutations were tested with respect to their activity at $\alpha6/\alpha3\beta2\beta3$ and $\alpha3\beta2$ nAChRs. As seen in Table 3, each of these double mutants preferentially blocks the $\alpha6/\alpha3\beta2\beta3$ receptor versus the $\alpha3\beta2$ receptor. The IC_{50} of the MII[H9A;L15A] analog was approximately 2000-fold lower for $\alpha6/\alpha3\beta2\beta3$ versus $\alpha3\beta2$, and this analog was selected for further characterization (Fig. 3).

Kinetics of Block by MII[H9A;L15A]. α-Conotoxin MII is slowly reversible on $\alpha3\beta2$ nAChRs and very slowly reversible on $\alpha6/\alpha3\beta2\beta3$ nAChRs (Fig. 4). Substitution of Ala for His9 or Leu15 leads to more rapid recovery from block for both receptor subtypes. In the case of the double mutant MII[H9A;L15A] recovery from toxin block is rapid. The magnitude of the change of recovery rate is greater than the magnitude of change in IC_{50} at the $\alpha6/\alpha3\beta2\beta3$ receptor. This implies that changes in the peptide that lead to a rapid off-rate also lead to a faster on-rate of binding. We note that α-conotoxin GIC, a more rapidly reversible homolog of α-conotoxin MII, also has an alanine rather than the histidine found in position 9 of α-MII (McIntosh et al., 2002).

Activity of MII[H9A;L15A] on Other nAChR Subtypes. MII[H9A;L15A] has highest affinity for the $\alpha6/\alpha3\beta2\beta3$ subunit combination and ~100-fold less activity on the $\alpha6/\alpha3\beta4$ combination (Fig. 3). MII[H9A;L15A] has low or no activity on the remaining neuronal subunit combinations tested, including $\alpha2\beta2$, $\alpha2\beta4$, $\alpha3\beta4$, $\alpha4\beta2$, $\alpha4\beta4$, and $\alpha7$ (Fig. 5 and Table 4). Thus, MII[H9A;L15A] selectively blocks $\alpha6$* nAChRs, with preference for the $\alpha6/\alpha3\beta2\beta3$ versus $\alpha6/\alpha3\beta4$ subunit combination.

Effect of $\beta3$ Subunit. Occasional expression of $\alpha6/\alpha3\beta2$ was seen without coinjection of the $\beta3$ subunit. MII[H9A;L15A] blocked $\alpha6/\alpha3\beta2$ nAChRs with an IC_{50} of 8.21 (6.36–10.6) nM compared with 2.4 nM (1.68–3.43) for $\alpha6/\alpha3\beta2\beta3$. As indicated above (Fig. 2 and Table 2), MII[E11A] blocked $\alpha6/\alpha3\beta2$ nAChRs with an IC_{50} of 0.154 nM (0.134–0.178) compared with 0.16 nM (0.135–0.189) on $\alpha6/\alpha3\beta2\beta3$ nAChRs. Numbers in parentheses are 95% confidence intervals.

Activity of Analogs at Native Mouse Brain nAChRs. A concentration-response analysis was performed on four of the analogs with $\alpha6/\alpha3$* versus $\alpha3$* selectivity—MII[H9A], MII[E11A], MII[L15A], and MII[H9A;L15A]—using inhibition of [^{125}I]α-conotoxin MII binding (Whiteaker et al., 2000b) to mouse brain homogenates. Results are shown in Fig. 6. The values obtained for these analogs correlate well with values obtained on $\alpha6/\alpha3\beta2\beta3$ rather than $\alpha3\beta2$ nAChRs as expressed in *X. laevis* oocytes (Table 5).

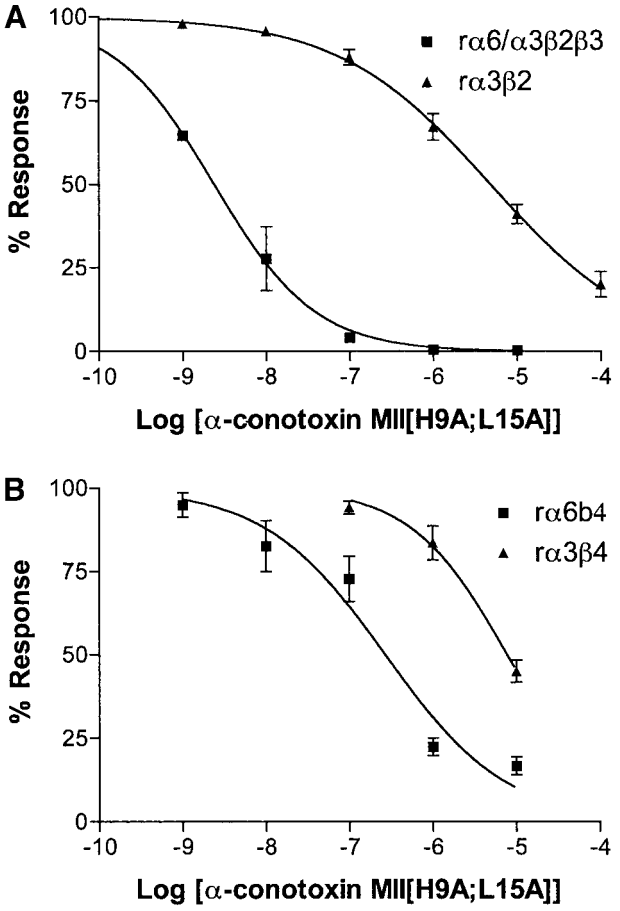

Fig. 3. The [H9A,L15A] analog of α-MII discriminates between $\alpha6$* and $\alpha3$* nAChRs. Peptide was applied to oocytes expressing the indicated nAChR subunit combinations as described under *Materials and Methods*. A, the peptide blocked rat $\alpha3\beta2$ with an IC_{50} of 4.8 μM (CI = 3.5–6.6 μM) and n_H of 0.48 ± 0.04. The peptide blocked rat $\alpha6/\alpha3\beta2\beta3$ with an IC_{50} of 2.4 nM (CI = 1.7–3.4 nM) and n_H of 0.72 ± 0.09. B, the peptide blocked rat $\alpha3\beta4$ with an IC_{50} of 7.8 μM (CI = 5.3–11.5 μM) and n_H of 0.75 ± 0.1. The peptide blocked rat $\alpha6\beta4$ with an IC_{50} of 269 nM (CI = 153–476 nM) and n_H of 0.60 ± 0.09; ± values are standard error of the mean.

Discussion

Although the sequence of the coding region for the $\alpha6$ gene has been known for many years (Lamar et al., 1990), its functional significance has been challenging to elucidate because of difficulties in heterologously expressing $\alpha6$ and because of a lack of subtype-specific ligands. Indeed, originally it was not entirely certain that the $\alpha6$ gene encoded a nicotinic receptor subunit. The $\alpha6$ subunit has relatively discrete localization, with expression in catacholaminergic nuclei including the locus coeruleus, the ventral tegmental area, and

the substantia nigra (Le Novère et al., 1996; Göldner et al., 1997; Han et al., 2000; Quik et al., 2000; Azam et al., 2002). It is also found in trigeminal ganglion and olfactory bulb (Keiger and Walker, 2000). In addition, α6 complexes have been reported in chick retina (Vailati et al., 1999). The α6 mRNA expression pattern overlaps extensively with that of

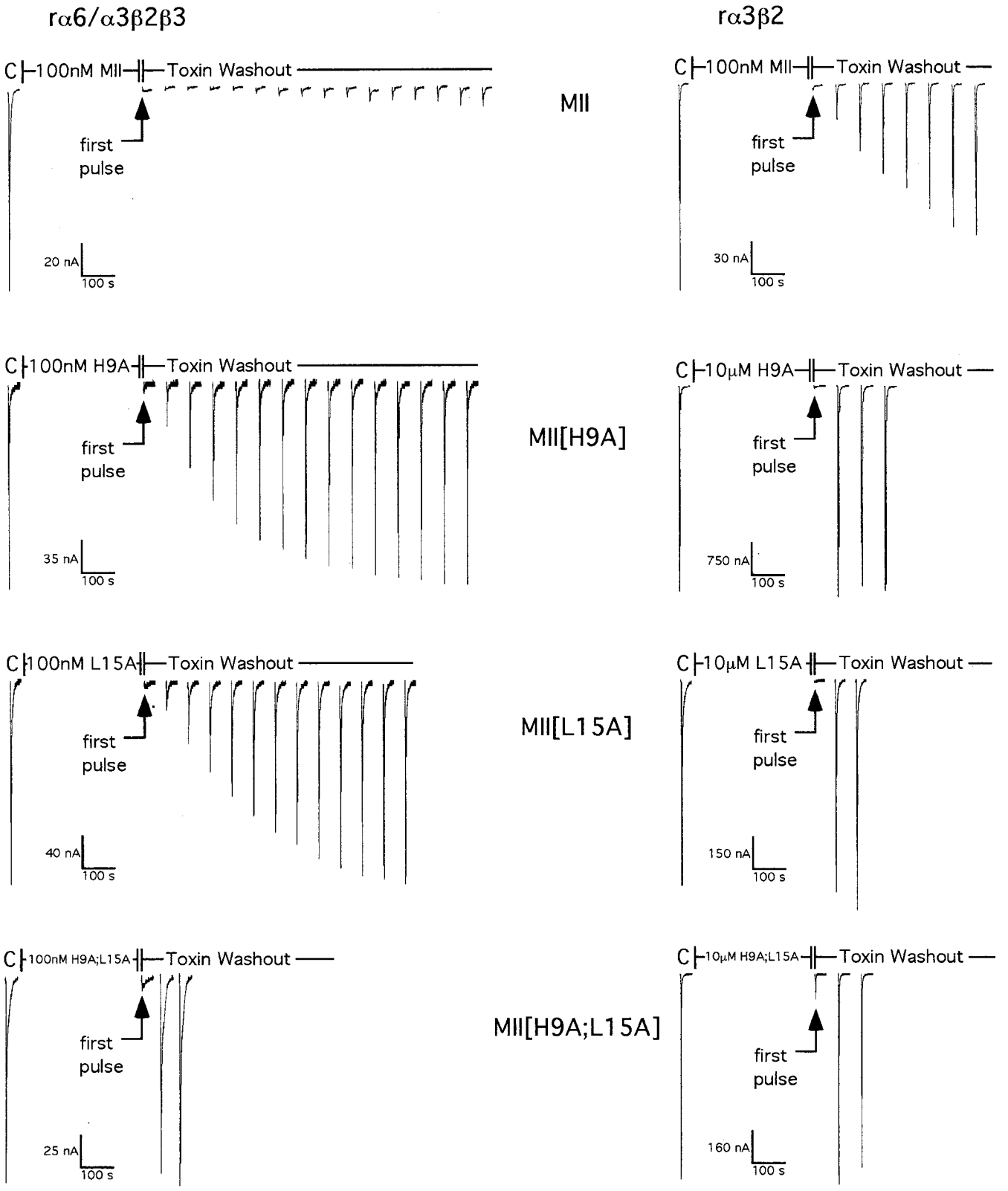

Fig. 4. Kinetics of block. MII, MII[H9A], MII[L15A], and MII[H9A;L15A] were applied to *X. laevis* oocytes heterologously expressing rat α6/α3β2β3 and α3β2 nAChRs. Peptide at the indicated concentrations was bath-applied for 5 min and then washed out. Kinetics of unblock were monitored by applying a 1-s pulse of ACh every 1 min.

the α3 subunit, leading to initial confusion over the composition of [^{125}I]α-conotoxin MII-binding nAChRs (Whiteaker et al., 2000b).

Subunit-specific antibodies have been used to immunoprecipitate α6* receptors from chick retina. When reconstituted in lipid bilayers, these receptors formed cationic channels characteristic of nAChRs, thus establishing a functional role for native α6* nAChRs (Vailati et al., 1999). Antibodies have also been used recently to demonstrate the presence of α6β2* nAChRs in striatal dopaminergic terminals in rat. β3 and/or α4 subunits are also present in a proportion of these nAChRs (Zoli et al., 2002). Subunit knockout mice suggest that the high-affinity binding site of [^{125}I]α-conotoxin MII is predominately composed of α6* rather than α3* nAChRs (Champtiaux et al., 2002; Whiteaker et al., 2002). It has been hypothesized recently that putative α6* nAChRs in the striatum may participate in the pathophysiology of Parkinson's disease, a neurodegenerative disorder characterized by progressive loss of dopamine neurons. Treatment of primates with 1-methyl-4-phenyl-1,2,3,6-tetrahydropyridine (a dopaminergic neurotoxin) leads to selective decline of putative α6β2* nAChRs (Quik et al., 2001; Kulak et al., 2002). Thus, there is a significant need for ligands that selectively act at α6* nAChRs.

We demonstrate in this report that certain analogs of α-conotoxin MII exhibit preferential loss of activity at α3β2 versus α6/α3β2β3 nAChRs. Additionally, at concentrations tested, the MII[H9A;L15A] analog has little or no activity at α2*, α4*, or α7* nAChRs. Indeed, MII[H9A;L15A] is the most selective α6 ligand thus far reported.

A number of native α-conotoxins have been characterized that target various subtypes of nAChRs. Despite their differences in primary sequence, NMR and X-ray crystallography studies show a high conservation of the structural peptide backbone (Hu et al., 1996, 1997, 1998; Shon et al., 1997; Hill et al., 1998; Cho et al., 2000; Park et al., 2001; Nicke et al., 2003). It seems that this backbone serves as a scaffold that presents a variety of amino acid side chains leading to differences in specificity. In the present study, we have systematically replaced the noncysteine residues of α-conotoxin MII with alanine. The predominant effect is to preferentially decrease activity at the α3β2 receptor relative to the α6/α3β2($\pm\beta$3) subunit combination.

In an attempt to further increase selectivity, double mutations were constructed from the more selective single mutation analogs. Each of these double mutants retains a low nanomolar IC_{50} for the α6/α3β2β3 nAChR (Table 3). It is particularly noteworthy that the native MII peptide potently blocks both α6/α3β2β3 and α3β2 nAChRs, whereas the MII[H9A;L15A] analog discriminates between these nAChRs by three orders of magnitude. This discrimination is caused by differences in the extracellular region of the α subunit because the transmembrane and intracellular portions of the chimeric α6/α3 and α3 subunits are identical. Also, the addition of the β3 subunit to α6/α3β2 nAChRs has only a 3.4-fold effect on MII[H9A,L15A] block. MII[E11A] also preferentially blocks α6/α3β2 versus α3β2 nAChRs, again implicating the extracellular portion of the α6 subunit. Furthermore, coexpression of the β3 subunit with the α6/α3 and β2 subunits had no effect on the IC_{50} of MII[E11A]. However, the presence of a β2 versus β4 subunit does seem to influence peptide affinity. MII[E11A] preferentially blocks α6/α3β2 versus α6/α3β4 nAChRs and preferentially blocks α3β2 versus α3β4 nAChRs.

We used cloned rat receptor subunits heterologously expressed in *X. laevis* oocytes to examine the differences between α3* and α6* nAChRs. Although difficult, occasional expression of α6 with either β2 or β4 subunits has been described. This expression is enhanced with the addition of the β3 subunit (Kuryatov et al., 2000). Improved efficiency of expression has been achieved by combining the extracellular (putative ligand binding) domain of α6 with the remaining

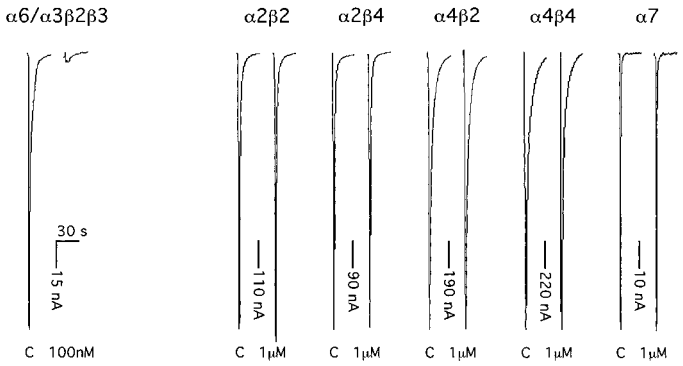

Fig. 5. Effects of MII[H9A,L15A] on additional nAChR subtypes. Peptide at 100 nM (α6/α3β2β3) and 1 μM (all other subtypes) was bath-applied for 5 min to *X. laevis* oocytes expressing the indicated rat nAChR subunits. Traces are representative of experiments on three to five oocytes. C, control response to ACh. Second response in each trace pair is the response to ACh in the presence of peptide.

TABLE 4
Effects of MII[H9A;L15A]
Values are the percentage of control ± S.E.M.

Receptor	Concentration of MII[H9A; L15A]	
	10 μM	1 μM
Rα2β2	102 ± 1.4	103 ± 1.9
Rα2β4	96.7 ± 3.2	95.9 ± 2.3
Rα4β2	98.5 ± 4.4	101 ± 2.5
Rα4β4	99.0 ± 4.0	100 ± 5.6
Rα7	61.4 ± 2.3	100 ± 1.5

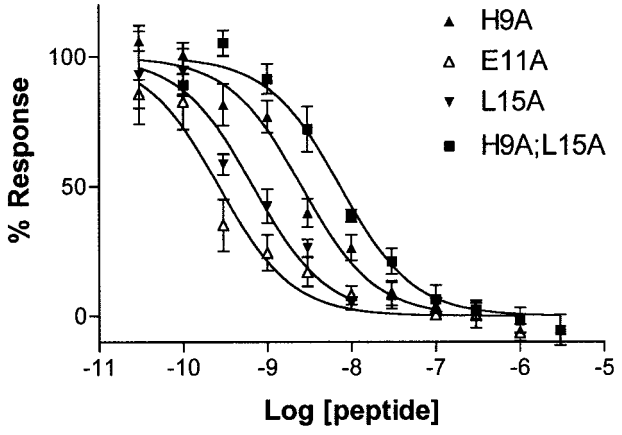

Fig. 6. Concentration-response analysis of α-conotoxin MII analogs on native nAChRs. Analogs were assessed for their ability to displace [^{125}I]α-conotoxin MII binding on mouse brain homogenates as described under *Materials and Methods*. Nonspecific binding was defined with 1 μM epibatidine. K_i values are shown in Table 5. The Hill slope was 0.95 ± 0.13, 0.89 ± 0.14, and 1.1 ± 0.14 for MII[H9A], MII[L15A], and MII[H9A;L15A], respectively. ± values are standard error of the mean. Data are from three to seven experiments.

TABLE 5

α -Conotoxin MII and analogs

Rat nAChRs were heterologously expressed in oocytes, and functional block of ACh-induced current was measured. Radioiodinated α -conotoxin MII was used with mouse brain homogenates to examine the competition binding of the indicated peptides. See Figs. 1, 2, 3, and 6. Numbers in parentheses are 95% confidence intervals.

Peptide	IC_{50} Rat α3β2	IC_{50} Rat α6/α3β2β3	K_i Mouse CNS α-MII Site
		nM	
α-MII	2.2 (1.2–3.8)	0.39 (0.28–0.55)	0.22 (0.20–0.25)
MII[H9A]	59 (44–79)	0.79 (0.56–1.1)	1.1 (0.84–1.6)
MII[E11A]	8.7 (6.8–11.1)	0.16 (0.13–0.19)	0.27 (0.19–0.37)
MII[L15A]	34 (19–60)	0.92 (0.65–1.3)	0.30 (0.21–0.45)
MII[H9A;L15A]	4800 (3500–6600)	2.4 (1.7–3.4)	3.3 (2.5–4.3)

portion of either the α3 or α4 subunit (Kuryatov et al., 2000). We have exploited this technique to screen analogs of α-conotoxin MII. It is possible that there are important differences between this chimeric receptor expressed in oocytes and native nAChRs. To assess this, the α-conotoxin MII analogs were also tested in a radioligand binding assay using native nAChR populations. As can be seen in Table 5, the analogs that potently block the rat α6/α3β2β3 nAChR heterologously expressed in oocytes also potently block the native mouse striatal nAChR bound by radiolabeled MII. This native receptor has been shown in previous studies to contain α6 (rather than α3) and β2 subunits (Champtiaux et al., 2002; Whiteaker et al., 2002; Zoli et al., 2002). Thus, the analogs have high affinity for both native and heterologously expressed α6β2* nAChRs. The H9A;L15A analog of MII also has a relatively high IC_{50} for other nAChRs, including α2β2, α2β4, α3β2, α3β4, α4β2, α4β4, and α7. Thus, this peptide represents a novel selective probe for discriminating among numerous nAChR subunit combinations.

The precise mechanism by which the [H9A] and [L15A] mutations cause a selective loss of affinity at α3β2 relative to α6/α3β2* nAChRs is not addressed by these studies. It has been determined that Lys185 and Ile188 of the α3 subunit are critically important for α-conotoxin MII binding to α3β2 nAChRs (Harvey et al., 1997), and these residues are conserved between the α3 and α6 subunits. The most facile explanation of the results presented here is that the crucial interactions between α-conotoxin MII and the α6 subunit may occur at other subunit side chains. Interestingly, both α-conotoxin PnIA and α-conotoxin MII interact with Ile188 but differ in other important interactions with the α3 subunit. α3 subunit Lys185 is not essential to α-conotoxin PnIA binding, whereas Pro182 and Gln198 are (Everhart et al., 2003). Perhaps significantly, the latter two residues are not conserved between the α3 and α6 subunit. Because all of the above residues are found in the putative "C" loop of the α subunit, it seems possible that interaction in this region may be of particular importance. However, several examples indicate that a more complex explanation may be needed. For instance, α-conotoxin PnIA and its derivative α-conotoxin PnIA[A10L] stabilize different states of the same nAChR (Hogg et al., 2003), presumably by interacting with different sets of subunit residues, whereas α-conotoxin MI has been shown to interact in a different orientation with the same α1 subunit residues, depending on whether it is binding at an α/γ or α/δ interface (Sugiyama et al., 1998). These and a series of mutant-cycle analysis studies (Quiram et al., 1999, 2000; Bren and Sine, 2000) have indicated that toxin/channel interactions may be anchored by a small number of relatively strong interactions and supported by a large number of weaker interactions that strongly determine subtype selectivity (Rogers et al., 2000). If this more multifaceted model is correct, the maintenance of affinity between α-conotoxin MII[H9A;L15A] and the α6/α3β2* nAChR may reflect either a more prominent role of the "supporting" interactions with the native toxin than is seen for α3β2, which is retained after alteration of the His9 and Leu15 side chains. Alternatively, the orientation of the toxin within the binding pocket may shift after substitution at the His9 and Leu15 positions, but the structure of the α6/α3 binding pocket may be better able to accommodate the new positioning than its α3 counterpart. The fact that several of the alanine mutants exhibit affinities similar to each other and native α-conotoxin MII but have radically different binding kinetics reinforces the idea that different interactions may stabilize the nAChR/toxin complex in each case. It seems likely that an accurate understanding of how the [H9A] and [L15A] mutations produce selectivity between α3β2 and α6/α3β2* nAChRs will require the performance of a comprehensive set of double mutant-cycle analyses.

Acknowledgments

Mass spectrometry was performed by W. Low and A.G. Craig of the Salk Institute. We thank Sean Christensen for providing technical support.

References

Azam L, Winzer-Serhan UH, Chen Y, and Leslie FM (2002) Expression of neuronal nicotinic acetylcholine receptor subunit mRNAs within midbrain dopamine neurons. *J Comp Neurol* **444:**260–274.

Bren N and Sine SM (2000) Hydrophobic pairwise interactions stabilize α-conotoxin MI in the muscle acetylcholine receptor binding site. *J Biol Chem* **275:**12692–12700.

Cartier GE, Yoshikami D, Gray WR, Luo S, Olivera BM, and McIntosh JM (1996) A new α-conotoxin which targets α3β2 nicotinic acetylcholine receptors. *J Biol Chem* **271:**7522–7528.

Champtiaux N, Han Z-Y, Bessis A, Rossi FM, Zoli M, Marubio L, McIntosh JM, and Changeux J-P (2002) Distribution and pharmacology of α6-containing nicotinic acetylcholine receptors analysed with mutant mice. *J Neurosci* **22:**1208–1217.

Changeux J-P (1993) Chemical signaling in the brain. *Sci Am* **269:**58–62.

Cheng YC and Prusoff WH (1973) Relationship between the inhibition constant (K_i) and the concentration of inhibitor which causes 50% inhibition (IC_{50}) of an enzymatic reaction. *Biochem Pharmacol* **22:**3090–3108.

Cho JH, Mok KH, Olivera BM, McIntosh JM, Park KH, and Han KH (2000) Nuclear magnetic resonance solution conformation of α-conotoxin AuIB, an α3β4 subtype-selective nicotinic acetylcholine receptor antagonist. *J Biol Chem* **275:**8680–8685.

Corringer PJ, Le Novere N, and Changeux J-P (2000) Nicotinic receptors at the amino acid level. *Annu Rev Pharmacol Toxicol* **40:**431–458.

Cui C, Booker TK, Allen RS, Grady SR, Whiteaker P, Marks MJ, Salminen O, Tritto T, Butt CM, Allen WR, et al. (2003) The β3 nicotinic receptor subunit: a component of α-conotoxin MII binding nAChRs which modulate dopamine release and related behaviors. *J Neurosci* **23:**11045–11053.

Deneris ES, Boulter J, Swanson LW, Patrick J, and Heinemann S (1989) Beta3: A new member of the nicotinic acetylcholine receptor gene family is expressed in the brain. *J Biol Chem* **264:**6268–6272.

Everhart D, Reiller E, Mirzoian A, McIntosh JM, Malhotra A, and Luetje CW (2003) Identification of residues that confer α-conotoxin PIA sensitivity on the α3 subunit of neuronal nicotinic acetylcholine receptors. *J Pharmacol Exp Ther* **306:**665–670.

Göldner FM, Dineley KT, and Patrick JW (1997) Immunohistochemical localization of the nicotinic acetylcholine receptor subunit α6 to dopaminergic neurons in the substantia nigra and ventral tegmental area. *Neuroreport* **8:**2739–2742.

Han Z-Y, Le Novère N, Zoli M, Hill JA Jr, Champtiaux N, and Changeux J-P (2000) Localization of nAChR subunit mRNAs in the brain of *Macaca mulatta*. *Eur J Neurosci* **12:**3664–3674.
Harvey SC, McIntosh JM, Cartier GE, Maddox FN, and Luetje CW (1997) Determinants of specificity for α-conotoxin MII on α3β2 neuronal nicotinic receptors. *Mol Pharmacol* **51:**336–342.
Hill JM, Oomen CJ, Miranda LP, Bingham JP, Alewood PF, and Craik DJ (1998) Three-dimensional solution structure of α-conotoxin MII by NMR spectroscopy: effects of solution environment on helicity. *Biochemistry* **37:**15621–15630.
Hogg RC, Hopping G, Alewood PF, Adams DJ, and Bertrand D (2003) α-Conotoxin PnIA and [A10L]PnIA stabilize different states of the α7-L247T nicotinic acetylcholine receptor. *J Biol Chem* **278:**26908–26914.
Hu S-H, Gehrmann J, Alewood PF, Craik DJ, and Martin JL (1997) Crystal structure at 1.1 Å resolution of α-conotoxin PnIB: comparison with α-conotoxins PnIA and GI. *Biochemistry* **36:**11323–11330.
Hu SH, Gehrmann J, Guddat LW, Alewood PF, Craik DJ, and Martin JL (1996) The 1.1 Å crystal structure of the neuronal acetylcholine receptor antagonist, α-conotoxin PnIA from *Conus pennaceus*. *Structure* **4:**417–423.
Hu S-H, Loughnan M, Miller R, Weeks CM, Blessing RH, Alewood PF, Lewis RJ, and Martin JL (1998) The 1.1 Å resolution crystal structure of [Tyr15]EpI, a novel α-conotoxin from *Conus episcopatus*, solved by direct methods. *Biochemistry* **37:**11425–11433.
Keiger CJ and Walker JC (2000) Individual variation in the expression profiles of nicotinic receptors in olfactory bulb and trigeminal ganglion and identification of α2, α6, α9 and β3 transcripts. *Biochem Pharmacol* **59:**233–240.
Kulak JM, McIntosh JM, and Quik M (2002) Loss of nicotinic receptors in monkey striatum after 1-methyl-4-phenyl-1,2,3,6-tetrahydropyridine treatment is due to a decline in α-conotoxin MII sites. *Mol Pharmacol* **61:**230–238.
Kuryatov A, Olale F, Cooper J, Choi C, and Lindstrom J (2000) Human α6 AChR subtypes: subunit composition, assembly and pharmacological responses. *Neuropharmacology* **39:**2570–2590.
Lamar D, Miller K, and Patrick J (1990) Amplification of genomic sequences identified in new gene, a6, in the nicotinic acetylcholine receptor gene family. *Soc Neurosci Abstr* **16:**2852.
Le Novère N, Zoli M, and Changeux JP (1996) Neuronal nicotinic receptor α6 subunit mRNA is selectively concentrated in catecholaminergic nuclei of the rat brain. *Eur J Neurosci* **8:**2428–2439.
Le Novère N, Zoli M, Lèna C, Ferrari R, Picciotto MR, Merlo-Pich E, and Changeux J-P (1999) Involvement of α7 nicotinic receptor subunit in nicotine-elicited locomotion, demonstrated by *in vivo* antisense oligonucleotide infusion. *Neuroreport* **10:**2497–2501.
Luo S, Kulak JM, Cartier GE, Jacobsen RB, Yoshikami D, Olivera BM, and McIntosh JM (1998) α-Conotoxin AuIB selectively blocks α3β4 nicotinic acetylcholine receptors and nicotine-evoked norepinephrine release. *J Neurosci* **18:**8571–8579.
Luo S, Nguyen TA, Cartier GE, Olivera BM, Yoshikami D, and McIntosh JM (1999) Single-residue alteration in α-conotoxin PnIA switches its nAChR subtype selectivity. *Biochemistry* **38:**14542–14548.
Luo Z, Fuentes M-E, and Taylor P (1994) Regulation of acetylcholinesterase mRNA stability by calcium during differentiation from myoblasts to myotubes. *J Biol Chem* **269:**27216–27223.
McIntosh JM, Dowell C, Watkins M, Garrett JE, Yoshikami D, and Olivera BM (2002) α-Conotoxin GIC from *Conus geographus*, a novel peptide antagonist of nAChRs. *J Biol Chem* **277:**33610–33615.
Nicke A, Loughnan ML, Millard EL, Alewood PF, Adams DJ, Daly NL, Craik DJ, and Lewis RJ (2003) Isolation, structure and activity of GID, a novel 4/7α-conotoxin with an extended N-terminal sequence. *J Biol Chem* **278:**3137–3144.
Park KH, Suk J-E, Jacobsen R, Gray WR, McIntosh JM, and Han KH (2001) Solution conformation of α-conotoxin EI, a neuromuscular toxin specific for the α1/δ subunit interface of *Torpedo* nicotinic acetylcholine receptor. *J Biol Chem* **276:**49028–49033.
Quik M, Polonskaya Y, Gillespie A, Jakowec M, Lloyd GK, and Langston JW (2000) Localization of nicotinic receptor subunit mRNAs in monkey brain by in situ hybridization. *J Comp Neurol* **424:**58–69.
Quik M, Polonskaya Y, Kulak JN, and McIntosh JM (2001) Vulnerability of ^{125}I-α-conotoxin MII binding sites to nigrostriatal damage in monkeys. *J Neurosci* **21:**5494–5500.
Quiram PA, Jones JJ, and Sine SM (1999) Pairwise interactions between neuronal α7 acetylcholine receptors and α-conotoxin ImI. *J Biol Chem* **274:**19517–19524.
Quiram PA, McIntosh JM, and Sine SM (2000) Pairwise interactions between neuronal α7 acetylcholine receptors and α-conotoxin PnIB. *J Biol Chem* **275:**4889–4896.
Rogers JP, Luginbuhl P, Pemberton K, Harty P, Wemmer DE, and Stevens RC (2000) Structure-activity relationships in a peptide α7 nicotinic acetylcholine receptor antagonist. *J Mol Biol* **304:**911–926.
Shon K, Koerber SC, Rivier JE, Olivera BM, and McIntosh JM (1997) Three-dimensional solution structure of α-conotoxin MII, an α3β2 neuronal nicotinic acetylcholine receptor-targeted ligand. *Biochemistry* **36:**15693–15700.
Sugiyama N, Marchot P, Kawanishi C, Osaka H, Molles B, Sine SM, and Taylor P (1998) Residues at the subunit interfaces of the nicotinic acetylcholine receptor that contribute to α-conotoxin MI binding. *Mol Pharmacol* **53:**787–794.
Vailati S, Hanke W, Bejan A, Barabino B, Longhi R, Balestra B, Moretti M, Clementi F, and Gotti C (1999) Functional α6-containing nicotinic receptors are present in chick retina. *Mol Pharmacol* **56:**11–19.
Whiteaker P, Jimenez M, McIntosh JM, Collins AC, and Marks MJ (2000a) Identification of a novel nicotinic binding site in mouse brain using [^{125}I]-epibatidine. *Br J Pharmacol* **131:**729–739.
Whiteaker P, McIntosh JM, Luo S, Collins AC, and Marks MJ (2000b) ^{125}I-α-Conotoxin MII identifies a novel nicotinic acetylcholine receptor population in mouse brain. *Mol Pharmacol* **57:**913–925.
Whiteaker P, Peterson CG, Xu W, McIntosh JM, Paylor R, Beaudet AC, Collins AC, and Marks MJ (2002) The role of the α3 subunit in neuronal nicotinic binding populations. *J Neurosci* **22:**2522–2529.
Zoli M, Moretti M, Zanardi A, McIntosh JM, Clementi F, and Gotti C (2002) Identification of the nicotinic receptor subtypes expressed on dopaminergic terminals in the rat striatum. *J Neurosci* **22:**8785–8789.

Address correspondence to: Dr. J. Michael McIntosh, University of Utah, Department of Biology, 257 South 1400 East, Salt Lake City, UT 84112. E-mail: mcintosh@biology.utah.edu